Protein Arms in the Kinetochore-Microtubule Interface of the Yeast DASH Complex

Molecular Biology of the Cell
Vol. 18, 2503–2510, July 2007

Protein Arms in the Kinetochore-Microtubule Interface of the Yeast DASH Complex[D]

JJ L. Miranda,*† David S. King,‡ and Stephen C. Harrison§

*Department of Molecular and Cellular Biology, Harvard University, Cambridge, MA 02138; ‡Department of Molecular and Cell Biology, and Howard Hughes Medical Institute, University of California, Berkeley, CA 94720; and §Department of Biological Chemistry and Molecular Pharmacology, and Howard Hughes Medical Institute, Harvard Medical School, Boston, MA 02115

Submitted February 16, 2007; Revised April 10, 2007; Accepted April 17, 2007
Monitoring Editor: Kerry Bloom

The yeast DASH complex is a heterodecameric component of the kinetochore necessary for accurate chromosome segregation. DASH forms closed rings around microtubules with a large gap between the DASH ring and the microtubule cylinder. We characterized the microtubule-binding properties of limited proteolysis products and subcomplexes of DASH, thus identifying candidate polypeptide extensions involved in establishing the DASH-microtubule interface. The acidic C-terminal extensions of tubulin subunits are not essential for DASH binding. We also measured the molecular mass of DASH rings on microtubules with scanning transmission electron microscopy and found that approximately 25 DASH heterodecamers assemble to form each ring. Dynamic association and relocation of multiple flexible appendages of DASH may allow the kinetochore to translate along the microtubule surface.

INTRODUCTION

Division of one parental cell into two genetically identical progeny requires accurate partitioning of newly replicated chromosomes. Of the many protein assemblies that monitor, regulate, and drive this process, only the kinetochore directly contacts centromeric DNA. In yeast kinetochores, over 60 proteins assemble into distinct subcomplexes on a ~125-base pair centromere to bind a single microtubule (MT) of the mitotic spindle (McAinsh *et al.*, 2003). Structural studies of these subcomplexes coupled with functional experiments have begun to add molecular detail to our picture of kinetochores. For example, the yeast Ndc80 complex forms a 570-Å coiled coil rod with two globular domains at each end (Wei *et al.*, 2005), suggesting a role as a molecular adaptor. The globular domain of the human Ndc80 subunit, Hec1, folds into a MT-binding calponin homology domain (Wei *et al.*, 2007), and the worm Ndc80 homolog directly binds MTs and facilitates association of additional kinetochore complexes (Cheeseman *et al.*, 2006). The yeast DASH complex (also called the Dam1 complex) forms closed rings around MTs (Miranda *et al.*, 2005). DASH can be induced to move along a MT and to translate with the depolymerizing end (Westermann *et al.*, 2005, 2006). The interaction resists several picoNewtons of force (Asbury *et al.*, 2006). DASH may therefore serve to help tether kinetochores to MTs during chromosome segregation.

This article was published online ahead of print in *MBC in Press* (http://www.molbiolcell.org/cgi/doi/10.1091/mbc.E07–02–0135) on April 25, 2007.

[D] The online version of this article contains supplemental material at *MBC Online* (http://www.molbiolcell.org).

† Present address: Department of Cellular and Molecular Pharmacology, University of California, San Francisco, CA 94158.

Address correspondence to: Stephen C. Harrison (harrison@crystal.harvard.edu).

The DASH complex is necessary for faithful segregation of chromosomes in mitosis. The *Saccharomyces cerevisiae* complex consists of 10 essential subunits: Dam1p, Duo1p, Dad1p, Dad2p, Spc19, Spc34p, Ask1p, Dad3p, Dad4p, and Hsk3p (Figure 1A) (Cheeseman *et al.*, 2001, 2002; Janke *et al.*, 2002; Li *et al.*, 2002, 2005). Loss of functional DASH results in sister chromatids attached to the same spindle pole body, an arrangement that leads to unequal segregation. The homologous complex in *Schizosaccharomyces pombe* contains similar subunits and localizes to kinetochores as well as to MT plus ends (Liu *et al.*, 2005; Sanchez-Perez *et al.*, 2005). Although not essential in fission yeast, loss of functional DASH also results in segregation defects. The ring structure observed in vitro may contribute to proper segregation by acting as a processivity factor for kinetochores, allowing chromosomes to remain attached to depolymerizing MT plus ends during anaphase. Rings are commonly found in assemblies that must remain attached to a linear substrate, for example, in the assemblies that carry out DNA replication (Hingorani and O'Donnell, 2000). The mechanism by which the DASH ring binds to and translates along MTs is therefore not only an integral part of how kinetochores work, but also an instance of a molecular solution to a ubiquitous structural challenge.

Negative stain electron microscopy (EM) of MTs decorated with DASH reveals a gap between the inner diameter of DASH and the outer diameter of the MT (Miranda *et al.*, 2005; Westermann *et al.*, 2005, 2006). No discrete mass of DASH can be seen abutting the MT, but polypeptide extensions not visibly contrasted by negative stain may position DASH rings around microtubules. On the MT side, the acidic C-termini of tubulin may project from the surface, but the 10–20 amino acids of these unstructured extensions (Lowe *et al.*, 2001) are unlikely to bridge the 50–100-Å gap of the DASH-MT interface. Because rotary shadowed EM preparations show that DASH is relatively compact, but hydrodynamic measurements yield a Stokes' radius much larger

than expected for a globular particle (Miranda *et al.*, 2005), we believe that extended projections are probably present. No obvious candidates for those bridging elements can be deduced from examination of amino acid sequences of DASH components. We have therefore carried out a series of experiments to determine the location and MT-binding properties of flexible, protease-sensitive polypeptides on DASH. This mapping adds detail to models of how DASH binds to and translates along MTs.

MATERIALS AND METHODS

Cloning

Constructs of *S. cerevisiae* DASH or subcomplexes were cloned into a polycistronic coexpression system (Miranda *et al.*, 2005). The plasmid containing Ask1p with a C-terminal Strep-tag was generated in an analogous manner. Constructs without *HSK3* were obtained by omitting the subcloning step incorporating *HSK3* from pET21aTr into the expression vector. This procedure was repeated to generate similar plasmids encoding Ask1p, Dad1p, Dad2p, Dad3p, Dad4p, Spc19p, and Spc34p with C-terminal hexahistidine tags. A construct without *DAM1* was obtained by omitting the subcloning step incorporating *DAM1* from pET3aTr into the expression vector. This procedure generated a plasmid encoding Spc34p with a C-terminal hexahistidine tag and Ask1p with a C-terminal Strep-tag. Vectors with only *DAD1* and *DAD3* were generated by sequentially subcloning *DAD1* and *DAD3* from pET3aTr into the compatible restriction sites of the first and third cassettes in pST39 as NheI/BamHI and SacI/KpnI fragments, respectively. This procedure was repeated to generate similar plasmids encoding Dad1p and Dad3p with C-terminal hexahistidine tags.

Protein Expression and Purification

DASH complexes were purified with combinations of affinity, ion exchange, and size-exclusion chromatography (Miranda *et al.*, 2005). DASH subcomplexes were purified in the same manner as heterodecameric DASH containing a protein with a C-terminal hexahistidine tag except that the ion exchange column and peptide treatments were omitted. DASH containing Ask1p with a C-terminal Strep-tag was purified in a similar manner with modifications. Cells were lysed in 50 mM phosphate, 500 mM NaCl, 1 mM mercaptoethanol, 1 mM EDTA, 1 mM phenylmethylsulfonyl fluoride (PMSF), and Complete Protease Inhibitors (Roche, Indianapolis, IN), pH 7.5. The supernatant was bound to a Strep-Tactin Sepharose (IBA, St. Louis, MO) column and washed in the same buffer without protease inhibitors but including 1 mM ATP and 0.1 mg/ml of the synthetic peptide NRLLLTG. The complex was eluted in the wash buffer supplemented with 2.5 mM desthiobiotin. The eluant was concentrated, fresh ATP added to 1 mM, and additional NRLLLTG peptide added to 250-fold molar excess relative to the DASH. The complex was then purified on a Superose 6 10/300 column (Amersham, Piscataway, NJ) equilibrated in 25 mM HEPES, 500 mM NaCl, 1 mM mercaptoethanol, and 1 mM EDTA, pH 7.4.

Microtubule Decoration

Bovine tubulin was polymerized in the presence of paclitaxel (Miranda *et al.*, 2005). MT cosedimentation assays were performed by mixing 10 μl of 1 mg/ml DASH or subcomplex in 25 mM HEPES, 500 mM NaCl, 1 mM mercaptoethanol, 1 mM EDTA, pH 7.4, with 90 μl of 0.055 mg/ml MTs in 25 mM HEPES, 100 mM NaCl, 1 mM GTP, 10 mM paclitaxel, and 1% dimethyl sulfoxide (DMSO), pH 7.4. Control samples were treated with buffer instead of DASH or subcomplex. All samples were incubated for 20 min at room temperature and then spun at 16,000 $\times$ *g* for 10 min at room temperature.

Limited Proteolysis

DASH at 1 mg/ml and elastase (Sigma, St. Louis, MO) at 0.1 mg/ml, both in 25 mM HEPES, 500 mM NaCl, 1 mM mercaptoethanol, and 1 mM EDTA, pH 7.4, were mixed at a ratio of 9:1. Reactions were incubated at 4°C and quenched by the addition of SDS-PAGE buffer and boiling. The initial time-point sample was treated with buffer instead of elastase. For further purification, 500 μl of DASH proteolyzed for 30 min was fractionated on a Superose 6 10/300 column (Amersham) equilibrated in 25 mM HEPES, 500 mM NaCl, 1 mM mercaptoethanol, and 1 mM EDTA, pH 7.4. For experiments testing the ability of MTs to protect DASH against elastase digestion, 0.05 mg/ml MTs decorated with 0.1 mg/ml DASH was mixed with 0.01 mg/ml elastase in 25 mM HEPES, 150 mM NaCl, 1 mM GTP, 10 μM paclitaxel, 1% DMSO, pH 7.4, at room temperature. The initial time-point sample was treated with buffer instead of elastase. Control samples were treated with buffer instead of MTs. For subtilisin treatment of MTs, 9 vol of polymerized MTs at 5 mg/ml were mixed with 1 vol of 2 mg/ml subtilisin (Sigma) in 80 mM PIPES, 1 mM $MgCl_2$, and 1 mM EGTA, pH 6.9. The reaction was incubated at 30°C for 60 min (Skiniotis *et al.*, 2004), quenched by the addition of 10 mM PMSF from a 100 mM stock in ethanol, spun at 16,000 $\times$ *g* for 10 min, and resuspended in 25 mM HEPES, 100 mM NaCl, 1 mM GTP, 10 μM paclitaxel, 1% DMSO, and 1 mM PMSF, pH 7.4. Control samples were treated with buffer instead of subtilisin. All subsequently used buffers contained 1 mM PMSF. Western blots verifying cleavage of the C-terminus of β-tubulin were probed with the mAb JDR.3B8 (Sigma), which is specific for that epitope (Banerjee *et al.*, 1988). Similarly, cleavage of the C-terminus of α-tubulin was verified by probing with the mAb YL1/2 (AbD Serotec, Raleigh, NC), which is specific for the C-terminal tyrosine residue (Wehland *et al.*, 1984).

Phosphorylation In Vitro

One vol of DASH at 1 mg/ml in 25 mM HEPES, 500 mM NaCl, 1 mM mercaptoethanol, 1 mM EDTA, pH 7.4, and 1 vol of human Cdc2-cyclin B (New England Biolabs, Beverly, MA) in 50 mM HEPES, 100 mM NaCl, 1 mM dithiothreitol, 100 μM EDTA, 50% glycerol, and 0.01% Brij 35, pH 7.5, 1 vol of 500 mM Tris, 100 mM $MgCl_2$, 20 mM dithiothreitol, 10 mM EGTA, 50% glycerol, and 0.1% Brij 35, pH 7.5, and 1 vol of 2 mM ATP were diluted into water to a total of 10 vol. Alternatively, 2 vol of human Cdk2-cyclin A (New England Biolabs) were substituted. Reactions were incubated at 4°C overnight. Control samples were treated with water instead of ATP. For gel electrophoresis, samples were quenched by the addition of SDS-PAGE buffer and boiling. EM and mass spectrometry (MS) experiments were performed with reactions including human Cdk2-cyclin A and DASH containing Spc34p with a C-terminal His-tag.

Mass Spectrometry

Peptide maps of proteins in gel bands were obtained by in-gel trypsinolysis and peptide extraction using conventional methods and analysis by matrix-assisted laser desorption ionization time-of-flight MS (Bruker, Billerica, MA). Intact proteins were desalted by polystyrene-divinylbenzene microbore reversed-phase liquid chromatography, and intact masses were measured by matrix-assisted laser desorption ionization time-of-flight MS (Bruker) as well as by electrospray ionization-ion trap MS (Bruker-Agilent, Santa Clara, CA). Phosphorylation was assessed by microwave trypsinolysis (CEM, Matthews, NC) of the proteins of interest for 7 min with 25 W at 50°C followed by desalting on a ZipTip (Millipore, Bedford, MA) and flow-injection analysis of the entire tryptic digest on a 9.4-T electrospray ionization-Fourier transform ion cyclotron resonance mass spectrometer (Bruker).

Electron Microscopy

Negatively stained specimens of decorated MTs were prepared with uranyl formate (Miranda *et al.*, 2005). Samples of MTs decorated by DASHΔHsk3p 6mer contained 0.1 mg/ml MTs and 0.2 mg/ml DASHΔHsk3p 6mer. Samples of MTs decorated by DASH modified by Cdk were prepared by mixing 5.5 μl of 5 mg/ml MTs in 74 mM PIPES, 1 mM GTP, 1 mM $MgCl_2$, 1 mM EGTA, 100 μM paclitaxel, and 7.5% DMSO, pH 6.9, to 50 μl of a kinase reaction. The sample was spun, resuspended, and then absorbed onto a grid. Scanning transmission electron microscopy (STEM) experiments were performed at Brookhaven National Laboratory. MTs at 0.05 mg/ml were partially decorated with 0.01 mg/ml DASH for observation of single rings (Miranda *et al.*, 2005). The grids were freeze-dried overnight and transferred into the microscope under vacuum. Digital dark-field images were obtained at an operating voltage of 40 kV. Control samples were treated with buffer instead of DASH. Experiments were performed with DASH containing Spc34p with a C-terminal His-tag. Data were analyzed with PCMASS29 (Wall and Simon, 2001), which performs background calculations to subtract from the summed intensity measurements. For analysis, each particle was chosen manually from a 5120 $\times$ 5120-Å scan with 10-Å spacing and centered in a 400 $\times$ 800-Å box. Two data sets were analyzed, one including all reasonably unencumbered particles based on visual inspection and a smaller collection including only particles that met more stringent visual criteria for background and proximity to other particles. Molecular masses were calibrated using a mass/length value of 13.1 kDa/Å for tobacco mosaic virus, which is included as a control on all grids.

RESULTS

Limited Proteolysis of DASH

We used limited proteolysis to probe for protein "arms" that could bridge the gap between DASH rings and the MT. Mild digestion of the intact heterodecamer with elastase, which cleaves C-terminal to aliphatic side chains, yields only eight strong bands (Figure 1A). The proteolysis product resulting from 30 min of treatment represents the most easily isolated kinetic end point, which we therefore used for subsequent experiments. Ask1p, Dam1p, and Duo1p are cleaved. MS identified the new species appearing between Duo1p and Spc19p as the N-terminal portion of Duo1p. We detected 74% of the Duo1p sequence when mapping peptides in a

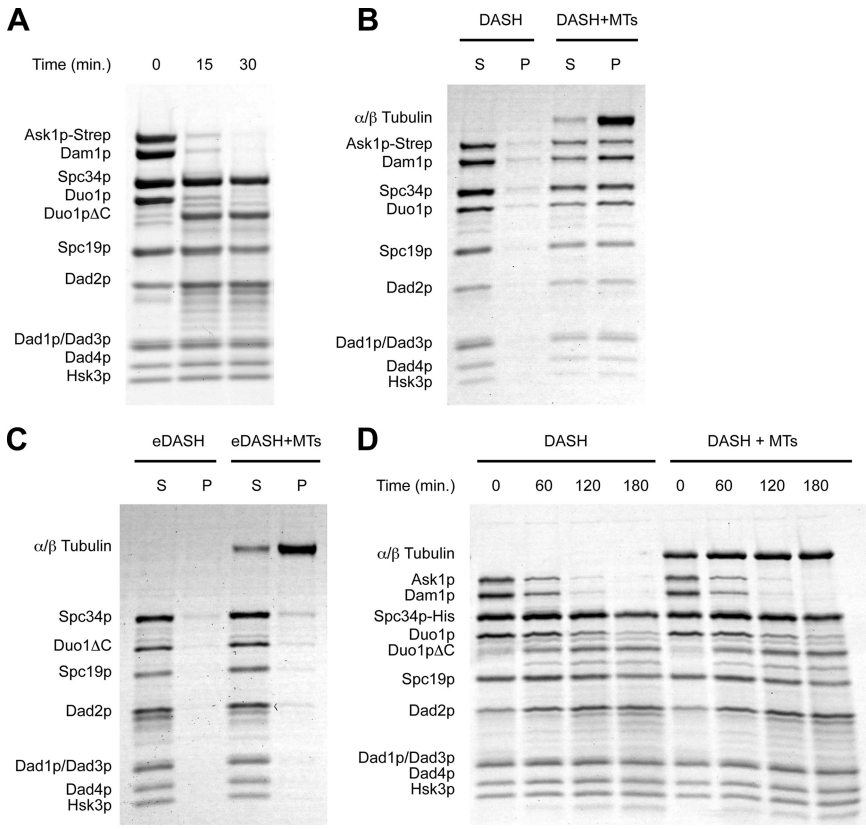

Figure 1. Biochemical properties of eDASH. (A) Time-dependent limited proteolysis treatment of DASH with elastase. (B) Cosedimentation assay of MTs with DASH. (C) Cosedimentation assay of MTs with eDASH. S and P, supernatant and pellet fractions, respectively. (D) Time-dependent limited proteolysis treatment of DASH with elastase in the absence and presence of MTs.

tryptic digestion of the band; the identified peptides spanned residues 2–212 of Duo1p, which has 247 residues total. Edman degradation yielded no sequences, a result explained by observation of an acetylated N-terminal peptide. A ladder of unsequenced bands that appears between Duo1p and Dad1p/Dad3p suggests that Dam1p and Ask1p have been cleaved into a number of different polypeptides. The low abundance and heterogeneity of the putative Dam1p and Ask1p proteolysis products has precluded identification. When further purified with size-exclusion chromatography (Supplementary Figure 1A), all eight components and the unsequenced cleavage products remained associated (Supplementary Figure 1B). We could detect no other globular complex of coeluting, protease-resistant protein. We refer to the purified product as elastase-treated DASH (eDASH).

Recombinant DASH binds MTs as judged by an in vitro MT cosedimentation assay (Figure 1B; Miranda *et al.*, 2005; Westermann *et al.*, 2005), but eDASH does not (Figure 1C). Nonetheless, MTs do not protect DASH from elastase digestion (Figure 1D). Moreover, the resulting eDASH, which is indistinguishable from eDASH prepared in the absence of MTs, no longer cosediments with MTs in the preparation (data not shown). We would expect contacts between the MT-bound heterodecamers within a ring to be shielded from proteolysis, but not dynamic, flexible extensions across the gap between the ring and MT. We believe that proteolysis eliminates direct DASH-MT interactions of this kind, thereby destabilizing the ring. An alternate possibility, that proteolysis destroys contacts between neighboring heterodecamers around the ring, is less consistent with the apparent lack of any protection from proteolysis in a MT-bound ring of DASH complexes relative to free DASH heterodecamer. We also note that eDASH tends to oligomerize at high concentrations during size-exclusion chromatography (data not shown), a property observed with DASH (Miranda *et al.*, 2005). This oligomerization suggests that the interface between eDASH heterodecamers within a ring may still be intact. Lack of protection of MT-bound DASH from proteolysis also suggests that either the contacting peptides are still exposed while bound to MTs or that the on and off rates of binding to MTs are high enough to free a reasonable fraction of the contacting peptides at any one moment. The width of the gap between the major mass of a DASH ring and the MT surface is 50–100 Å, so a polypeptide extension from a ring subunit might be easily accessible to elastase, an enzyme ~40–50 Å in diameter (Shotton and Watson, 1970), even when the tip of the extension is docked against the MT wall. Thus, the cleavage data suggest that exposed, extended parts of DASH bridge the ring and the MT lattice.

Microtubule Binding of DASH Subcomplexes

Characterization of the MT-binding properties of DASH subcomplexes suggests which proteins are likely to contribute extended arms to the MT-DASH interface. We have purified a variety of distinct subcomplexes by deleting different subunits from our coexpression vector (Miranda, 2006). DASHΔHsk3p 3mer, which contains Ask1p, Dad2p, and Dad4p (Figure 2A), does not cosediment with MTs (Figure 3A), but DASHΔHsk3p 6mer, which contains Dam1p, Duo1p, Spc34p, Spc19p, Dad1p, and Dad3p (Figure 2A), does (Figure 3B). The limited proteolysis experiments suggest Ask1p, Dam1p, and Duo1p as candidates for providing MT bridges. Because DASHΔHsk3p 3mer contains Ask1p and does not cosediment with MTs, we conclude that this subunit is not sufficient for establishing a functional DASH-MT interaction. DASHΔHsk3p 6mer contains both

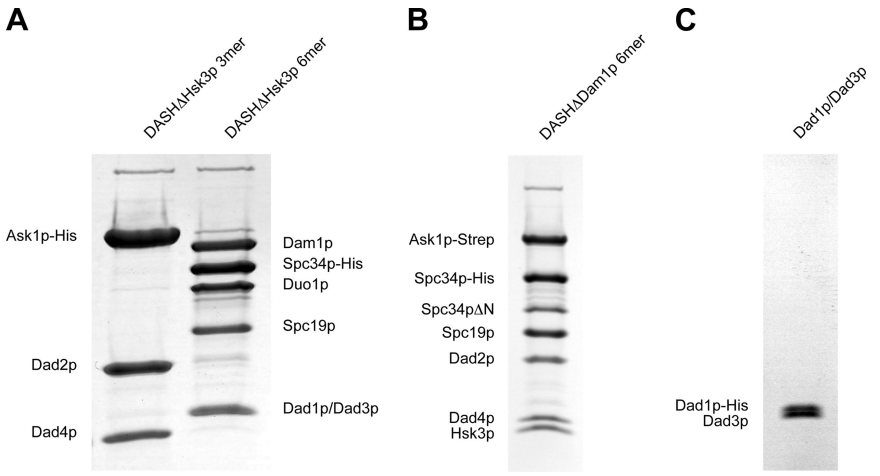

Figure 2. DASH subcomplexes. Purified recombinant (A) DASHΔHsk3p 3mer and 6mer subcomplexes, (B) DASHΔDam1p 6mer, and (C) Dad1p/Dad3p.

Dam1p and Duo1p, suggesting that the extensions cleaved by elastase on these two proteins are sufficient for association with MTs. Comparing EM images of undecorated (Figure 4A) and decorated MTs (Figure 4B) reveals an unorganized clustering of DASHΔHsk3p 6mer on the surface of the MT rather than organized rings. Extended elements of Dam1p, the C-terminus of Duo1p, or both are sufficient to form some interaction with MTs, but ring assembly and MT binding remain separable functions.

Lack of MT binding by other subcomplexes corroborates the importance of Dam1p and Duo1p in MT binding. DASHΔDam1p contains Ask1p, Spc34p, Spc19, Dad2p,

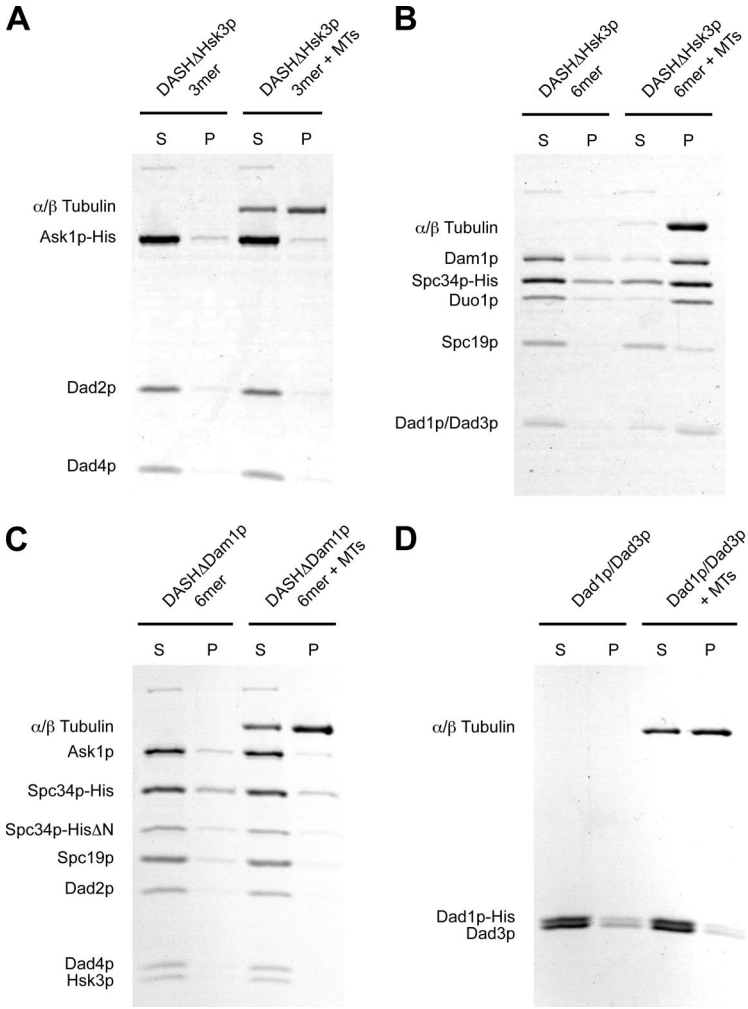

Figure 3. DASH subcomplex binding to MTs. Cosedimentation assays of MTs with (A) DASHΔHsk3p 3mer, (B) DASHΔHsk3p 6mer, (C) DASHΔDam1p 6mer, and (D) Dad1p/Dad3p. S and P, supernatant and pellet fractions, respectively.

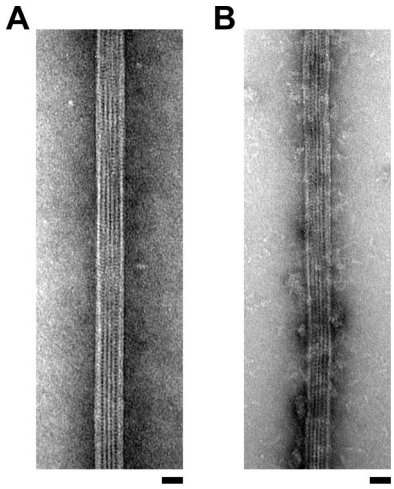

Figure 4. Negative stain EM micrographs of MT decoration by DASHΔHsk3p 6mer. Gallery of images showing a (A) MT and (B) MT with DASHΔHsk3p 6mer. Scale bars, 250 Å.

Dad4p, and Hsk3p (Figure 2B). MS analysis of the species between Spc34p and Spc19p identified 41% of Spc34p; mapped tryptic peptides spanned residues 99–274 out of 295. Edman degradation yielded the sequence MKRNRR, indicating that the observed band corresponds to an N-terminal truncation beginning at residue 93. The limited proteolysis experiments and MT cosedimentation assays of DASHΔHsk3p subcomplexes predict that DASHΔDam1p 6mer will not bind MTs, and we have confirmed this prediction (Figure 3C). During coexpression experiments, we also observed frequent overexpression of a Dad1p/Dad3p heterodimer relative to DASH (data not shown). The Dad1p/Dad3p heterodimer can be expressed and purified independently (Figure 2C). This subcomplex does not interact with MTs (Figure 3D), again consistent with previous conclusions. The absence of Dam1p, Duo1p, Dad1p, and Dad3p from DASHΔDam1p 6mer is noteworthy. Because Dad1p and Dad3p form a separable structural unit, Dam1p and Duo1p may form another distinct structural unit, a suggestion supported by their joint role in providing flexible extensions from MT interaction. The sum of the cosedimentation experiments is consistent with the interpretation that Dam1p and Duo1p cooperate to form the principal connection between DASH and MTs.

Limited Proteolysis of Microtubules

We have previously reported preliminary EM experiments suggesting that removal of the acidic C-termini of both α and β tubulin by subtilisin does not abolish DASH binding (Miranda *et al.*, 2005). The opposite conclusion has been drawn by others on the basis of EM and fluorescence binding assays (Westermann *et al.*, 2005). Our treatment of MTs with subtilisin alters electrophoretic mobility of both tubulin subunits on a gel (Figure 5A). Although this mobility shift is often a sufficient indicator of removal of both the α and β tubulin termini, we have also verified cleavage with epitope-specific monoclonal antibodies. The JDR.3B8 antibody detects the C-termini of β tubulin on mock-treated MTs, but not on subtilisin-treated MTs (Figure 5B). Similarly, the YL1/2 antibody detects the intact α subunit C-terminus, but almost all of the epitope is removed by subtilisin treatment (Figure 5C). DASH binds to subtilisin-digested MTs with similar affinity as it does to mock-digested MTs (Figure 5D). Moreover, we observe DASH rings with the same frequency on mock-treated (Figure 5E) and subtilisin-treated MTs (Figure 5F). The acidic C-termini of α and β tubulin are therefore not essential for proper formation of the DASH-MT interface, and we suggest that the flexible extensions of DASH dock against the cylindrical wall of the microtubule.

Phosphorylation of DASH

Ask1p is modified by a yeast cyclin-dependent kinase, Cdc28, in a cell cycle-dependent manner (Li and Elledge,

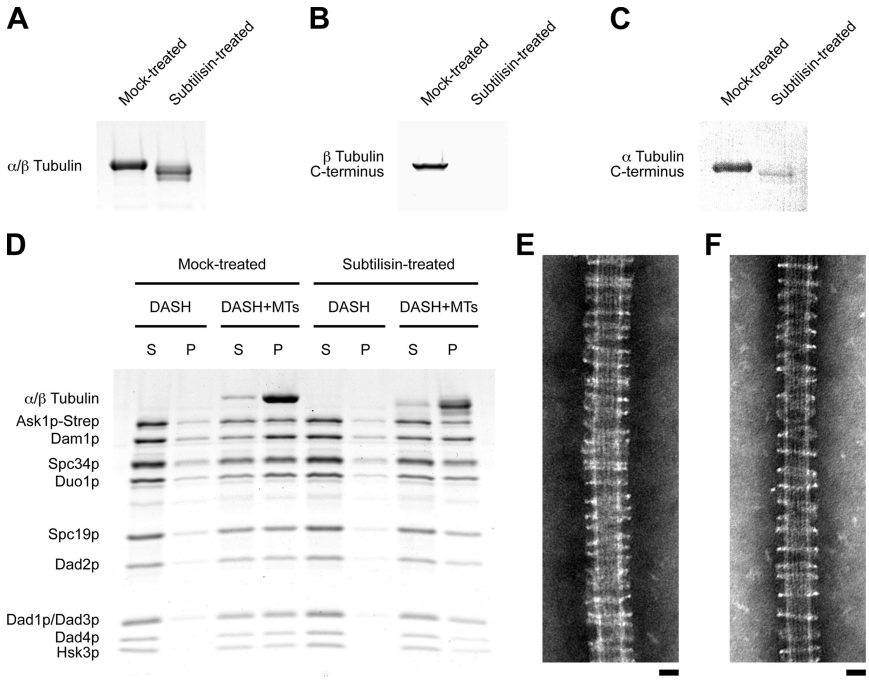

Figure 5. DASH binding to subtilisin-treated MTs. (A) Coomassie-stained gel of MT preparations. (B) Western blot of MT preparations probed with JDR.3B8, an antibody specific for the C-terminus of β tubulin. (C) Western blot of MT preparations probed with YL1/2, an antibody specific for the C-terminus of α tubulin. (D) Cosedimentation assay of subtilisin-treated MTs with DASH. S and P, supernatant and pellet fractions, respectively. (E) Negative stain EM micrograph of a mock-treated MT decorated by DASH. (F) Negative stain EM micrograph of a subtilisin-treated MT decorated by DASH. Scale bars, 250 Å.

2003), and mutation of both putative phosphorylation sites, S216 and S250, yields defects in anaphase spindle MT dynamics and chromosome segregation (Higuchi and Uhlmann, 2005). Incubation of DASH with Cdks in vitro results in a detectable electrophoretic mobility shift for only one component, Ask1p (Supplementary Figure 3, A and B). Time-of-flight MS of unmodified and modified Ask1p yields a molecular weight of 32058 (expected 32071) and 32132 (expected 32151) Da, respectively. The shift of 74 (expected 82) Da suggests that one and only one site is modified; no masses corresponding to unphosphorylated or diphosphorylated species are observed. Peptide mass mapping of modified Ask1p found the phosphorylated peptide QLAHEEHINNDGDNDDENSNNIESSPLK, which contains S250. The unphosphorylated form of the peptide was not found. A peptide containing S216, ISLLLQQQYGSSSSMVPSPIVPNK, is observed in the unphosphorylated state with no detection of a mass corresponding to the phosphorylated form. Phosphorylated DASH cosediments with MTs as efficiently as unphosphorylated DASH (data not shown). EM experiments also show that DASH phosphorylated by Cdk still forms rings around MTs with a similar frequency as does unphosphorylated DASH (data not shown). Cdks therefore modify DASH in vitro only on S250 of Ask1p, and this phosphorylation event does not affect ring assembly. We conclude that the anaphase defects seen when S250 is mutated must involve regulation of some other aspect of DASH activity.

Scanning Transmission Electron Microscopy

We have determined the molecular masses of MTs decorated with DASH rings by direct mass measurement with STEM. Substoichiometric amounts of DASH relative to tubulin were bound to MTs in order to favor the formation of single rings spaced sufficiently apart from each other to allow mass measurement of each particle. Unstained, lyophilized preparations were examined in the STEM. Images of particles from dark field micrographs were boxed into 400 × 800-Å arrays for analysis; high background as a result of binding conditions and specimen damage from mechanical manipulations resulted in only a small number of particles suitable for analysis. MTs appear as cylinders without the characteristic tubulin heterodimer repeat pattern probably because of radiation damage (Figure 6A). Our measurements of a 400-Å-long MT segment yielded a molecular mass of ~8 MDa (Table 1), close to the 7.8 MDa expected for a 14 protofilament MT. We performed similar measurements for MT segments decorated with DASH. MTs with single (Figure 6B) and double rings (Figure 6C) yielded molecular masses of ~13 and 18 MDa, respectively. The SD of our measurements ranged from 1 to 2 MDa, ~4–13% depending on the data set. The precision and accuracy of our measurements are similar to those obtained with kinesin-MT complexes (Hoenger *et al.*, 2000). We calculate the molecular mass of a ring as ~5 MDa, with propagated errors ranging from 0.5 to 2.5 MDa, ~10–60%, depending on the data set (Table 1). The molecular mass of one DASH heterodecamer is 0.2 MDa; each DASH ring therefore contains 25 ± 5 heterodecamers.

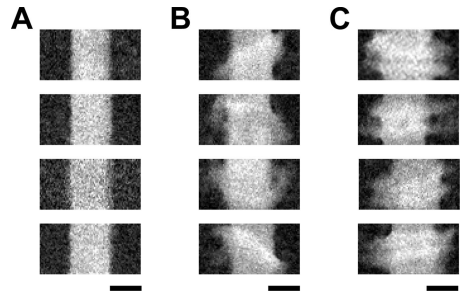

Figure 6. Dark field STEM micrographs of MT decoration by DASH. Gallery of images showing (A) MTs, (B) MTs with one DASH ring, and (C) MTs with two DASH rings. Scale bars, 250 Å.

Table 1. Molecular mass of DASH rings determined by STEM

Particle	N	Molecular mass (MDa)
MT	54 (32)[a]	8.4 ± 1.0 (7.9 ± 0.7)
MT and one DASH ring	24 (12)	13.6 ± 1.8 (12.4 ± 0.6)
MT and two DASH rings	23 (6)	18.2 ± 1.9 (18.0 ± 0.7)
(MT and one DASH ring) − (MT)[b]	n/a (n/a)	5.2 ± 2.0 (4.5 ± 0.9)
(MT and two DASH rings) − (MT and one DASH ring)[c]	n/a (n/a)	4.5 ± 2.5 (4.6 ± 0.9)
(MT and two DASH rings) − (MT)/2[d]	n/a (n/a)	4.9 ± 1.1 (5.1 ± 0.5)

[a] Results in parentheses obtained from a second data set with more stringent criteria used in picking particles for analysis.

[b] The difference between the measurements of MTs with one DASH ring and MTs.

[c] The difference between the measurements of MTs with two DASH rings and MTs with one DASH ring.

[d] Half the difference between the measurements of MTs with two DASH rings and MTs.

DISCUSSION

Chromosomes move along MTs during various stages of mitosis. In anaphase, progressive MT depolymerization at the plus end drives this translation so that net movement is toward the spindle pole body. We have proposed that the DASH rings are processivity factors that allow kinetochores to translate along a MT without dissociating (Miranda *et al.*, 2005), and the rings can indeed translate quite freely (Asbury *et al.*, 2006). The processivity factors that keep a DNA replication complex from dissociating slide loosely along the double helix (Hingorani and O'Donnell, 2000). A similar electrostatic sliding has been suggested for DASH (Westermann *et al.*, 2006), but the observations reported here lead us to seek an alternative mechanism. In particular, two results favor direct contacts. First, we find that the negatively charged tubulin C-termini on the MT surface do not appear to be essential for ring formation. Second, the DASHΔHsk3p 6mer subcomplex, which contains Dam1p and Duo1p, binds without forming rings. Were encirclement the only property holding DASH components onto a MT, we would expect ring formation to be essential for binding. We also note that sliding clamps in DNA replication need an energy-dependent clamp loader, whereas DASH rings assemble spontaneously around MTs.

Systematic analysis of the MT-binding properties of limited proteolysis products and various subcomplexes defines the nature of the DASH-MT interface. Polypeptide arms from both DASH and MTs could contribute to a molecular bridge across the gap observed between a DASH ring and the MT in EM images, but we determined that DASH alone makes functionally significant contacts across this space. Specifically, Dam1p, Duo1p, or both are probably responsible for MT binding (Figure 7A). Cleavage of these proteins

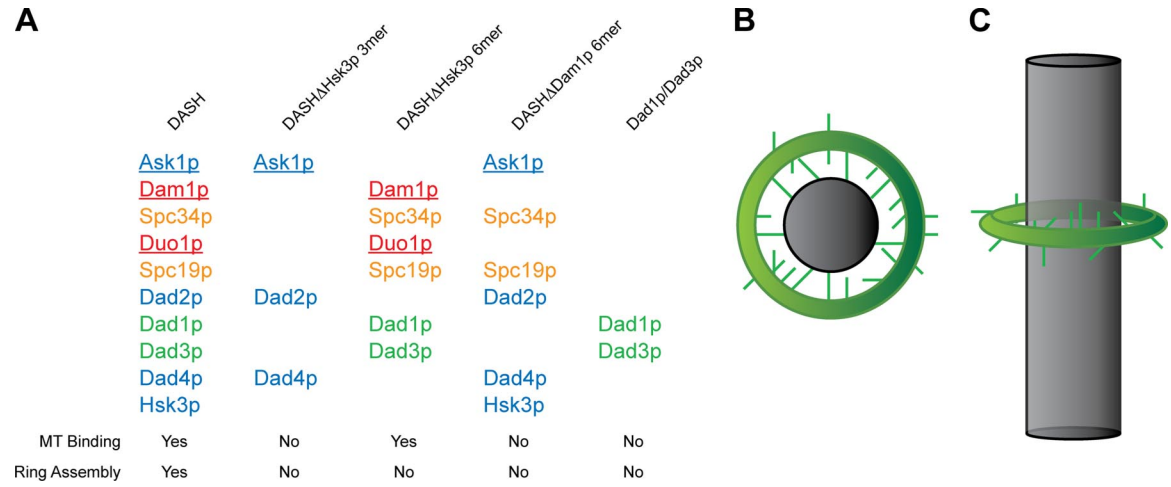

Figure 7. Functional organization of DASH. (A) Table depicting the compositions, MT binding properties, and ring assembly capabilities of DASH and subcomplexes. Underlines indicate proteins with flexible extensions as determined by limited proteolysis. Subunits are colored in groups defined by tendencies to appear and disappear together in different subcomplexes. (B) Schematic model of the interaction between a MT and DASH viewed along the MT axis. (C) The same model viewed orthogonal to the MT axis.

with elastase in limited proteolysis experiments abrogates the DASH-MT interaction; presence of these proteins in a subcomplex allows MT-binding. No other subunits meet both criteria. Our conclusion is consistent with previously reported observations from cosedimentation assays. In vitro–translated Dam1p binds MTs (Hofmann *et al.*, 1998), and a 138-amino acid truncation of the Dam1p C-terminus slightly lowers the affinity of recombinant DASH for MTs (Westermann *et al.*, 2005). Our experiments also show that upon removal of the acidic C-termini of both α and β tubulin, DASH still binds to and forms rings around MTs. A contrary conclusion was reached with different MT proteolysis protocols, cleavage verification methods, and binding assays (Westermann *et al.*, 2005); we cannot rationalize the difference in results. Our data suggest a DASH-MT interface in which extensions from DASH rings reach across a gap between the ring and MT and dock on the MT wall (Figure 7, B and C).

Our mass measurements indicate that each DASH ring contains ~20–30 heterodecamers, thereby defining the multiplicity of potential MT-binding contacts. This number is somewhat larger than other estimates. An apparent 16-fold symmetry of rare EM images of DASH bound to MTs led to the conclusion that rings contain 16 heterodecamers (Westermann *et al.*, 2006); the possibility of 32 copies was not considered. Fluorescence measurements of Ask1p copy number in vivo suggest 16–20 heterodecamers (Joglekar *et al.*, 2006). STEM is a direct measurement of the molecular mass of an isolated particle and depends on no assumptions other than appropriate calibration of the instrument. In any case, all the various measurements lead to the conclusion that the polyvalent DASH ring contains more sets of MT-binding extensions than the number of MT protofilaments.

We note that polyvalent attachment through extended arms or loops is fully compatible with diffusive motion, provided that the individual interactions are weak and that an individual arm may reach multiple tubulin docking sites. A range of potential attachment directions is consistent with the variable geometry with which DASH can decorate MTs in vitro, as rings and helices of various pitch. The lack of protection from proteolysis of Dam1p and Duo1p suggests that the cleavable extensions on these subunits are in dynamic equilibrium between the on and off positions. Indeed, all of the arms are unlikely to be engaged at once as the resulting avidity would probably yield too strong an attachment for translation along a MT. Thus, we imagine that at any moment only a fraction of the arms contact the MT. As the population of attached arms shifts, the ring will undergo diffusional translation along the MT, moving in one direction or the other at each step depending on whether a preponderance of the newly attaching arms lie toward one end or the other.

Molecular motors have been thought to move the kinetochore actively toward the poles during anaphase (Hyman *et al.*, 1992), but various lines of evidence suggest that motors are not essential in mitosis. Chromosome movement in *S. cerevisiae*, as measured by transient sister separation during metaphase, is unaffected by individual deletion of any of the nuclear kinesin-like motors (Tytell and Sorger, 2006). Poleward kinetochore movement in *S. pombe* during anaphase is unaffected by deletion all three known minus end–directed motors (Grishchuk and McIntosh, 2006). Experiments with chromosomes and MTs in vitro demonstrate that MT depolymerization alone is sufficient to drive chromosome segregation toward the MT minus end (Koshland *et al.*, 1988).

At least two models have been proposed to explain how MT depolymerization drives chromosome motion in anaphase. The conformational wave model (Koshland *et al.*, 1988) suggests that the curling of protofilaments at the depolymerizing end of a MT exerts force directly on the kinetochore, a process that propagates poleward. The diameter of the DASH ring would prevent it from falling off during depolymerization, making DASH a suitable force transducer (Miranda *et al.*, 2005; Westermann *et al.*, 2005). The biased-diffusion model (Hill, 1985) presumes that multiple attachment sites are present and that the energy required to move from one site on the MT lattice to another is sufficiently small to allow rapid diffusion of the kinetochore. At the depolymerizing plus end, new attachment sites are selectively available on one side of the ring and not the other, biasing diffusion toward the minus end. Curling could also contribute, especially if the docking sites were at the protofilament interface. Our picture of associating and dissociating bridges between the body of the DASH ring and the MT surface is compatible with either model.

ACKNOWLEDGMENTS

We thank members of the Brookhaven STEM, Cell Biology EM, and Howard Hughes Medical Institute mass spectrometry facilities for assistance with experiments. We also thank members of the Harrison laboratory for helpful discussions and Ian R. Levesque for computational support. The Brookhaven National Laboratory STEM is a National Institutes of Health Supported Resource Center, NIH 5 P41 EB2181, with additional support provided by the Department of Energy, Office of Biological and Environmental Research. J.L.M. was supported by a National Science Foundation Predoctoral Fellowship, and S.C.H. is an investigator of the HHMI.

REFERENCES

Asbury, C. L., Gestaut, D. R., Powers, A. F., Franck, A. D., and Davis, T. N. (2006). The Dam1 kinetochore complex harnesses microtubule dynamics to produce force and movement. Proc. Natl. Acad. Sci. USA *103*, 9873–9878.

Banerjee, A., Roach, M. C., Wall, K. A., Lopata, M. A., Cleveland, D. W., and Luduena, R. F. (1988). A monoclonal antibody against the type II isotype of beta-tubulin. Preparation of isotypically altered tubulin. J. Biol. Chem. *263*, 3029–3034.

Cheeseman, I. M., Anderson, S., Jwa, M., Green, E. M., Kang, J., Yates, J. R., 3rd, Chan, C. S., Drubin, D. G., and Barnes, G. (2002). Phospho-regulation of kinetochore-microtubule attachments by the Aurora kinase Ipl1p. Cell *111*, 163–172.

Cheeseman, I. M., Brew, C., Wolyniak, M., Desai, A., Anderson, S., Muster, N., Yates, J. R., Huffaker, T. C., Drubin, D. G., and Barnes, G. (2001). Implication of a novel multiprotein Dam1p complex in outer kinetochore function. J. Cell Biol. *155*, 1137–1145.

Cheeseman, I. M., Chappie, J. S., Wilson-Kubalek, E. M., and Desai, A. (2006). The conserved KMN network constitutes the core microtubule-binding site of the kinetochore. Cell *127*, 983–997.

Grishchuk, E. L., and McIntosh, J. R. (2006). Microtubule depolymerization can drive poleward chromosome motion in fission yeast. EMBO J. *25*, 4888–4896.

Higuchi, T., and Uhlmann, F. (2005). Stabilization of microtubule dynamics at anaphase onset promotes chromosome segregation. Nature *433*, 171–176.

Hill, T. L. (1985). Theoretical problems related to the attachment of microtubules to kinetochores. Proc. Natl. Acad. Sci. USA *82*, 4404–4408.

Hingorani, M. M., and O'Donnell, M. (2000). A tale of toroids in DNA metabolism. Nat. Rev. Mol. Cell Biol. *1*, 22–30.

Hoenger, A., Thormahlen, M., Diaz-Avalos, R., Doerhoefer, M., Goldie, K. N., Muller, J., and Mandelkow, E. (2000). A new look at the microtubule binding patterns of dimeric kinesins. J. Mol. Biol. *297*, 1087–1103.

Hofmann, C., Cheeseman, I. M., Goode, B. L., McDonald, K. L., Barnes, G., and Drubin, D. G. (1998). *Saccharomyces cerevisiae* Duo1p and Dam1p, novel proteins involved in mitotic spindle function. J. Cell Biol. *143*, 1029–1040.

Hyman, A. A., Middleton, K., Centola, M., Mitchison, T. J., and Carbon, J. (1992). Microtubule-motor activity of a yeast centromere-binding protein complex. Nature *359*, 533–536.

Janke, C., Ortiz, J., Tanaka, T. U., Lechner, J., and Schiebel, E. (2002). Four new subunits of the Dam1-Duo1 complex reveal novel functions in sister kinetochore biorientation. EMBO J. *21*, 181–193.

Joglekar, A. P., Bouck, D. C., Molk, J. N., Bloom, K. S., and Salmon, E. D. (2006). Molecular architecture of a kinetochore-microtubule attachment site. Nat. Cell Biol. *8*, 581–585.

Koshland, D. E., Mitchison, T. J., and Kirschner, M. W. (1988). Polewards chromosome movement driven by microtubule depolymerization in vitro. Nature *331*, 499–504.

Li, J. M., Li, Y., and Elledge, S. J. (2005). Genetic analysis of the kinetochore DASH complex reveals an antagonistic relationship with the ras/protein kinase A pathway and a novel subunit required for Ask1 association. Mol. Cell. Biol. *25*, 767–778.

Li, Y., Bachant, J., Alcasabas, A. A., Wang, Y., Qin, J., and Elledge, S. J. (2002). The mitotic spindle is required for loading of the DASH complex onto the kinetochore. Genes Dev. *16*, 183–197.

Li, Y., and Elledge, S. J. (2003). The DASH complex component Ask1 is a cell cycle-regulated Cdk substrate in *Saccharomyces cerevisiae*. Cell Cycle *2*, 143–148.

Liu, X., McLeod, I., Anderson, S., Yates, J. R., 3rd, and He, X. (2005). Molecular analysis of kinetochore architecture in fission yeast. EMBO J. *24*, 2919–2930.

Lowe, J., Li, H., Downing, K. H., and Nogales, E. (2001). Refined structure of alpha beta-tubulin at 3.5 A resolution. J. Mol. Biol. *313*, 1045–1057.

McAinsh, A. D., Tytell, J. D., and Sorger, P. K. (2003). Structure, function, and regulation of budding yeast kinetochores. Annu. Rev. Cell Dev. Biol. *19*, 519–539.

Miranda, J. J., De Wulf, P., Sorger, P. K., and Harrison, S. C. (2005). The yeast DASH complex forms closed rings on microtubules. Nat. Struct. Mol. Biol. *12*, 138–143.

Miranda, J. L. (2006). Structure of the Yeast DASH Complex, a Kinetochore-Microtubule Interface. Ph.D. Thesis. Cambridge, MA: Harvard University.

Sanchez-Perez, I., Renwick, S. J., Crawley, K., Karig, I., Buck, V., Meadows, J. C., Franco-Sanchez, A., Fleig, U., Toda, T., and Millar, J. B. (2005). The DASH complex and Klp5/Klp6 kinesin coordinate bipolar chromosome attachment in fission yeast. EMBO J. *24*, 2931–2943.

Shotton, D. M., and Watson, H. C. (1970). The three-dimensional structure of crystalline porcine pancreatic elastase. Philos. Trans. R. Soc. Lond. B Biol. Sci. *257*, 111–118.

Skiniotis, G., Cochran, J. C., Muller, J., Mandelkow, E., Gilbert, S. P., and Hoenger, A. (2004). Modulation of kinesin binding by the C-termini of tubulin. EMBO J. *23*, 989–999.

Tytell, J. D., and Sorger, P. K. (2006). Analysis of kinesin motor function at budding yeast kinetochores. J. Cell Biol. *172*, 861–874.

Wall, J. S., and Simon, M. N. (2001). Scanning transmission electron microscopy of DNA-protein complexes. Methods Mol. Biol. *148*, 589–601.

Wehland, J., Schroder, H. C., and Weber, K. (1984). Amino acid sequence requirements in the epitope recognized by the alpha-tubulin-specific rat monoclonal antibody YL 1/2. EMBO J. *3*, 1295–1300.

Wei, R. R., Al-Bassam, J., and Harrison, S. C. (2007). The Ndc80/HEC1 complex is a contact point for kinetochore-microtubule attachment. Nat. Struct. Mol. Biol. *14*, 54–59.

Wei, R. R., Sorger, P. K., and Harrison, S. C. (2005). Molecular organization of the Ndc80 complex, an essential kinetochore component. Proc. Natl. Acad. Sci. USA *102*, 5363–5367.

Westermann, S., Avila-Sakar, A., Wang, H. W., Niederstrasser, H., Wong, J., Drubin, D. G., Nogales, E., and Barnes, G. (2005). Formation of a dynamic kinetochore- microtubule interface through assembly of the Dam1 ring complex. Mol. Cell *17*, 277–290.

Westermann, S., Wang, H. W., Avila-Sakar, A., Drubin, D. G., Nogales, E., and Barnes, G. (2006). The Dam1 kinetochore ring complex moves processively on depolymerizing microtubule ends. Nature *440*, 565–569.